# Experimental measurement of focused wave group and solitary wave overtopping

# Experimental measurement of focused wave group and solitary wave overtopping

ALISON C. HUNT-RABY, Lecturer, *School of Marine Science and Engineering, University of Plymouth, Plymouth, PL4 8AA, U.K. Tel.: +44 1752 586133; fax: +44 1752 586101; e-mail: alison.raby@plymouth.ac.uk (author for correspondence)*

ALISTAIR G.L. BORTHWICK, Professor, *Department of Engineering Science, University of Oxford, Parks Road, Oxford OX1 3PJ, UK. Tel.: +44 1865 273047; fax: +44 1865 273010; e-mail: alistair.borthwick@eng.ox.ac.uk*

PETER K. STANSBY, Professor, *School of Mechanical, Aerospace and Civil Engineering, University of Manchester, PO Box 88, Manchester, M13 9PL, U.K. Tel.: +44 161 306 9202; fax: +44 161 306 4646;e-mail: peter.k.stansby@manchester.ac.uk*

PAUL H. TAYLOR, Professor, *Department of Engineering Science, University of Oxford, Parks Road, Oxford OX1 3PJ, UK. Tel.: +44 1865 273198; fax: +44 1865 273010; e-mail: paul.taylor@eng.ox.ac.uk*

## ABSTRACT

Prediction of individual wave overtopping events is important in assessing danger to life and property, but data are sparse and hydrodynamic understanding is lacking. Laboratory-scale waves of three distinct types were generated at the Coastal Research Facility to model extreme waves overtopping a trapezoidal embankment. These comprised wave groups of compact form, wave groups embedded in a background wave field, and a solitary wave. The inshore wave propagation was measured and the time variation of overtopping rate estimated. The total volume overtopped was measured directly. The experiments provide well defined data without uncertainty due to the effect of reflection on the incident wave train. The dependence of overtopping on a range of wave shapes is thus determined and the influence of wave-wave interactions on overtopping assessed. It was found that extreme overtopping may arise from focused waves with deep troughs rather than large crests. Further overtopping waves can be generated from small wave packets without affecting the applicability of results to cases where there are surrounding waves. Finally, overtopping from a solitary wave is surprisingly small compared with overtopping from focused wave groups of the same amplitude.

*Keywords*: Focused wave group, individual overtopping volume, overtopping volume estimation method, solitary wave, wave overtopping

## 1 Introduction

Wave overtopping of embankments and sea walls has received considerable attention in recent years. Coastal flood inundation due to wave overtopping of sea defences is of socioeconomic importance, with the likelihood of occurrence affected by rising sea levels due to climate and geological landform changes. Most research to date has concentrated on overtopping rates associated with storms, typically of three hours duration. Comprehensive design information is available in the Coastal Engineering Manual (Burcharth and Hughes 2006) and the EuroTop Manual (Pullen *et al*. 2007). The main parameters affecting the overtopping rate were found to be the significant wave height, peak spectral period of the underlying sea-state, crest freeboard and reducing factors were dependent on a berm, shallow foreshore, roughness, and angle of wave attack. A further influence is that of the breaker parameter, or surf similarity parameter $\xi = \tan\beta/(H_s/L_{op})^{1/2}$, which is a function of the structure slope $\tan\beta$ and wave steepness $H_s/L_{op}$, where $H_s$ is the significant wave height at the toe of the structure and $L_{op}$ the offshore wavelength $= gT_p^2/2\pi$, where $T_p$ is the peak period of the spectrum. The most widely accepted overtopping prediction formulae (Van der Meer and Janssen 1995) comprise two empirical equations for overtopping discharge, depending on whether or not the wave is breaking. The non-breaking form of the equation has no dependence of wave overtopping rate on wave steepness or structure slope.

Whereas the mean overtopping rate provides valuable information, data on individual wave overtopping are important for impacts on people and property and for causing lee-side erosion on embankments which may initiate breaching. Attempts have

been made to predict individual overtopping volumes, particularly maximum volumes, based upon assumed statistical distributions of overtopping volumes (Pullen *et al*. 2007, Besley 1999, Van der Meer and Janssen 1995). Few experimental studies were conducted on individual overtopping volumes. Tautenhain *et al*. (1982) used a video-system for measuring individual wave run-up and down-rush effects, as a basis for calculating overtopping rates. They found a strong correlation between experimental results and those obtained theoretically, using an energy conservation concept. Tsuruta and Goda (1968) generated regular and irregular waves, and measured the mean rates and individual volumes of vertical wall overtopping. Overtopping volumes of individual waves were estimated using a receptacle connected to a movable carriage via a load cell. By comparing the overtopping rates of regular and irregular waves of the same significant wave heights, Tsuruta and Goda (1968) observed that the overtopping rates of irregular waves were invariably smaller than those of regular waves, but these differences reduced as the wave height decreased. Tsuruta and Goda (1968) also estimated the individual overtopping volumes from irregular waves and compared them to overtopping volumes arising from regular waves. They found that there was good agreement for waves of the same incident crest height, though the data were scattered due to interference by preceding waves and some difficulties in measuring individual overtopped volumes.

Pearson *et al*. (2002) and Kortenhaus *et al*. (2004) used weighing cells to determine individual overtopping volumes. The latter found this technique to be more accurate than using either a wave gauge in an overtopping tank or a pair of pressure transducers at the floor of the tank.

Schüttrumpf and Oumeraci (2005) obtained individual overtopping volumes from the time integral of the overtopping rate, the rate being obtained from the product of overtopping layer thickness and overtopping velocity. They employed two methods to determine the velocity of the overtopping wave: directly with a micro-propeller and indirectly using the time taken for the wave to travel between two wave gauges. The time-of-flight technique between two gauges was widely used, for example by Richardson *et al*. (2002). However, this approach can only measure the leading edge jet velocity. As Schüttrumpf and Oumeraci (2005) explain, the highest velocity of the overturning jet occurs at its leading edge. Bosman *et al*. (2008) investigated discrepancies in the maximum flow depth and crest velocities presented separately by Schüttrumpf *et al*. (2001) and Van Gent (2002). Their main conclusion was that velocities measured during the large-scale tests by Schuttrümpf *et al*. (2001) were not always correct due to aerated flow, which was highly turbulent and non stationary. At full-scale, Troch *et al*. (2004) conducted field tests on a rubble mound breakwater in Zeebrugge, Belgium, using a large collection tank with a V-notch weir. Individual volumes were calculated, based upon assumed discharges over the weir and the time rate of change of water depth inside of the tank.

The effect of preceding waves on individual overtopping volumes is discussed in the literature but has not been specifically investigated. Tsurata and Goda (1968) recognised the effect of wave interference on overtopping volumes though they state that it plays a far less important role than wave height variability. Gunbak and Bruun (1979) provide a qualitative description of the effect of particular wave sequences interacting with rubble mound breakwaters. They predicted worst-case combinations of waves for overtopping and structure stability. They suggest that a modest amplitude wave of a particular period succeeded by a larger wave of shorter period will produce excessive overtopping, as the succeeding wave rides on the top of the preceding wave before it has had time to run down. Gunbak and Bruun (1979) also highlight the problems associated with deep troughs, indicating that if such a trough follows a small crest it can cause considerable run down with the potential for damage of the toe protection.

There remains a need for well-defined experimental data and understanding of overtopping due to individual waves in a random sea-state. In this research overtopping of a trapezoidal embankment by compact wave groups is considered, then, as a single comparison, overtopping by a solitary wave. The wave group which has become known as NewWave (Lindgren 1970, Tromans *et al*. 1991) is commonly used to represent the shape of extreme waves in a sea-state offshore, and here the NewWave is used as an input condition in intermediate depth. NewWave is a compact wave packet with a local time history identical to the scaled autocorrelation function, which is the Fourier transform of the spectrum of the assumed underlying random sea-state. This model was compared successfully to the average shape of large waves on the open sea for both deep water (Jonathan and Taylor 1997) and intermediate water depths (Taylor and Williams 2004). In this application the wave group is focused at various

distances offshore of the embankment. The aim is thus to understand wave-structure interactions in the overtopping process and to provide the time variation of overtopping rate without uncertainties due to reflections interacting with incoming waves.

The use of focused wave groups is novel in coastal engineering, though well-established in offshore engineering. Here it permits the detailed examination of individual extreme events, be they overtopping or run-up, of interest to the coastal engineering community by means of exactly repeatable experiments whilst avoiding the use of either long time domain random waves or regular waves. Incorporation of the NewWave approach into coastal engineering practice remains a topic of detailed investigation. Section 2 describes experimentation at the U.K. Coastal Research Facility, the instrumentation, mathematical definitions of the wave groups and their experimental realisation, and the methods used to estimate overtopping volumes. Section 3 presents the test results for global and local influences on individual overtopping events. Section 4 discusses the factors affecting individual wave overtopping. The findings are summarised in Section 5.

## 2 Method

### 2.1 *Experimental facility*

The wave overtopping experiments were carried out in the U.K. Coastal Research Facility (UKCRF), a basin with dimensions of 36 m alongshore by 20 m cross-shore. Waves were generated by a multi-element wave-maker, comprising 72 independently operated piston-type paddles. Each paddle was 1.5 m high and 0.5 m wide. The mean water depth at the paddles was 0.5 m. A flat bed extended about 8 m from the paddles to the toe of a 1:20 plane beach, with a seawall located near the shoreline (Figs. 1, 2).

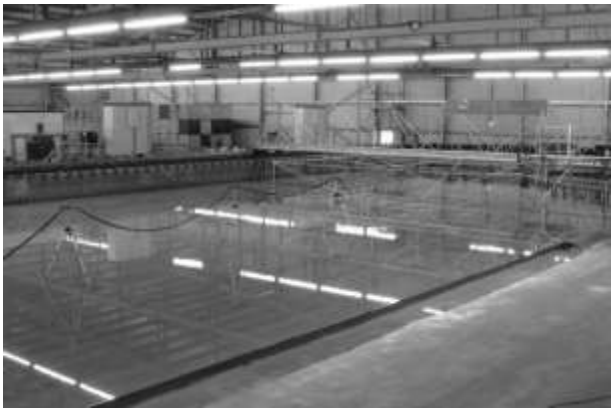

Figure 1 UK Coastal Research Facility

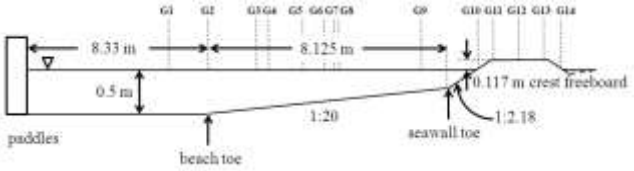


Figure 2 Schematic diagram of beach, seawall and selected gauge locations

The seawall stretched across the entire longshore basin dimension, and its toe was 8.125 m onshore of the beach toe. The central section of the wall had a horizontal crest and sloping back wall. The slope of the front face of the seawall to the horizontal was 1:2.18, which corresponds to a 1:2.5 slope for the front face of the seawall constructed on a 1:20 beach. The seawall either side of the central measurement section had a sloping face on the seaward side only. The framework of poles shown in the basin centre of Fig. 1 provided a support structure for up to 44 resistance-type wave gauges. All results presented here are taken from gauges along the centre-line (the onshore-offshore axis) of the basin.

### 2.2 *Wave generation*

The overtopping research programme considered 43 different wave conditions: focused wave groups, focused wave groups embedded within low-amplitude regular waves, and a solitary wave. The focused wave groups all had distinct properties governed by input amplitude, focus location, phase, angle of incidence, and long-crestedness. The choice of input wave amplitude was

governed by the maximum wave that could be generated at a particular location before breaking, in an effort to generate extreme amplitude waves. The tests presented here are for a sub-group of 13 normally-incident long-crested waves.

*Focused wave groups*

A focused wave group contains a range of individual linear sine wave components, each with an amplitude and frequency. The phase of each component was adjusted such that the crests of all the individual components coincide at a pre-selected position and time. Away from this point and instant, the composite wave system was lower in size and longer in duration because frequency dispersion results in different propagation speeds for each component. For these tests, a focused wave group based upon the NewWave concept (Tromans *et al*. 1991) was used which has a compact form with, in practice, only two or three waves generating overtopping for an input derived from a Pierson-Moskowitz spectrum. The choice of the spectrum is important because the amplitude spectrum of the compact wave group is matched to the energy spectrum for the supposed random sea from which the extreme wave packet is derived.

If the phase of all the wave group components at focus is shifted by $\pi$ radians then an inverted group can be generated, i.e. with a trough rather than a crest at focus. These crest- and trough-focused wave groups are illustrated in Fig. 3, which also shows the definitions of the intra-group wave numbering system (Wave I, II and III). The generation of crest- and trough-focused waves enables the influence of wave phase within the same (linear) wave packet shape on overtopping volume to be investigated since both wave groups illustrated in Fig. 3 have the same wave height though having different forms. It is worth noting that because the crest and trough-focused groups share the same wave envelope, they represent the arrival at the sea-wall of the same concentration of wave energy in each case.

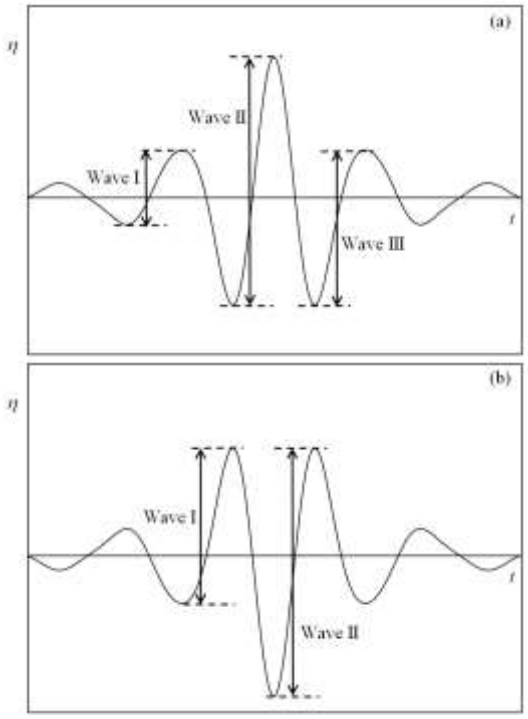


Figure 3 Definition of intra-group waves (a) crest-focused wave group, (b) trough-focused wave group

The surface elevation time history of a linear focused wave group is given by

$$\eta(x,t) = \sum_n a_n \cos(k_n x - \omega_n t + \varphi_n)$$

$$\eta(x,t) = \sum_n a_n \cos(k_n x - \omega_n t + \varphi_n) \qquad (1)$$

where $x$ is distance, $t$ time, $n$ the counter for the sum of the individual Fourier components combined to create the group, $a_n$ the wave amplitude, $k_n$ the wave number, $\omega_n$ the frequency and $\phi_n$ the phase angle of the $n$th component. For crest-focused waves $\phi_n = 0$, for trough-focused waves $\phi_n = \pi$, with the origins of both the distance and time scales being fixed at the focused wave event. The wave component amplitudes necessary to generate NewWave, a particular form of focused wave group, are given by

$$a_n = \frac{A_N S_n(\omega)\Delta\omega_n}{\sum_n S_n(\omega)\Delta\omega_n}$$

$$a_n = \frac{A_N S_n(\omega)\Delta\omega_n}{\sum_n S_n(\omega)\Delta\omega_n} \tag{2}$$

where $S_n(\omega)$ is the discretized energy spectrum, $\Delta\omega_n$ the frequency increment and $A_N = [2m_0(\ln(N)]^{1/2}$ where $m_0$ is the zero-th moment of the energy spectrum given by

$$m_0 = \sum_n S_n(\omega)\Delta\omega_n$$

$$m_0 = \sum_n S_n(\omega)\Delta\omega_n \tag{3}$$

and $N$ denotes the use of NewWave as a model for the largest in $N$ waves drawn from the assumed underlying random sea-state, assuming Rayleigh statistics for wave height. For a sea-state of 3 h, there could be ~1000 waves so a typical value would be $N$=1000. The relative distribution of wave amplitude across the individual frequency components thus mirrors the relative energy distribution across the assumed underlying wave spectrum (here Pierson-Moskowitz). In contrast, the amplitude of the NewWave is arranged such that the packet at focus contains one wave height (or linear crest) with a relative return period of 1 in $N$ waves within the sea-state, assuming the standard Rayleigh distribution for waves.

The paddle motion is related to Eq. (1) but with relative phase shifts to account for it creating wave components upstream and before the focus event. There is an additional $\pi/2$ phase shift, because the horizontal paddle velocity is in phase with wave crests, not the paddle displacement. The procedure also incorporates the paddle transfer functions which are deduced by carefully calibrating the wave basin for a range of amplitudes and frequencies (Dean and Dalrymple 1991). Note in passing that most experimental facilities would already have the modulus of the transfer function available, as this is required for random time-domain simulation. In order for NewWave-type experiments to be performed, both this modulus of the amplitude transfer function and the relative phase are required. The phase angle accounts for any phase shifts within the wave generation process and also for the time taken for a wave of given frequency to propagate from the paddle to the desired focus point within the wave tank.

*Embedded focused wave groups*

For the embedded group, the input amplitude of the regular wave train of 40.3 mm was selected assuming a typical three hour storm for the input of the focused group at this laboratory scale. The period of the regular wave of 1.747 s was related to the zero-crossing period of the wave group. A method proposed by Taylor *et al*. (1997) was used to embed the wave group into the regular wave. The basic idea behind the embedding of a large event is to mimic the random background within which an extreme wave would occur in a random sea-state. The rigorous analysis of Lindgren (1979) yields both the average shape of an extreme in a random process (NewWave) but also the possible variation of an individual record around the average shape when many extremes of this level are extracted from the assumed now very long record. Taylor *et al*. (1997) showed how to modify a short piece of random record by embedding an extreme event within it in such a way that simple statistical tests could not distinguish this

synthetic extreme event from an extreme in the original process. Herein, NewWave groups are embedded within a regular wave background. The variance (or standard deviation or $H_s$ value) for this regular train is the same as that for the Pierson-Moskowitz sea-state from which the 1 in 3 h extreme NewWave event itself is supposed to have been drawn. Hence in a crude sense, the regular background represents a series of average waves. To examine the phase effect of the regular wave train on overtopping due to the compact wave group, a total of four different embedded waves were generated:

1. Focused wave crest coincident with regular wave crest (EG1),

2. Focused wave trough coincident with regular wave crest (EG2),

3. Focused wave crest coincident with regular wave trough (EG3),

4. Focused trough coincident with regular wave trough (EG4).

EG1 and EG4 were therefore in phase at focus, and EG2 and EG3 were $\pi$ out of phase. Figure 4 compares the embedded focused group with the corresponding lone wave group. Close agreement between the shape of the dominant peaks and troughs of the embedded and lone wave groups is noted, with slightly reduced troughs in the crest-focused wave, and slightly reduced crests in the trough-focused wave. It is just discernable from Fig. 4 that the focus occurs just before the theoretical focal time for linear waves, $t = 0$ s. This is to be expected, and is due to the fact that the wave group exhibits non-linear characteristics as detailed by Baldock *et al*. (1996).

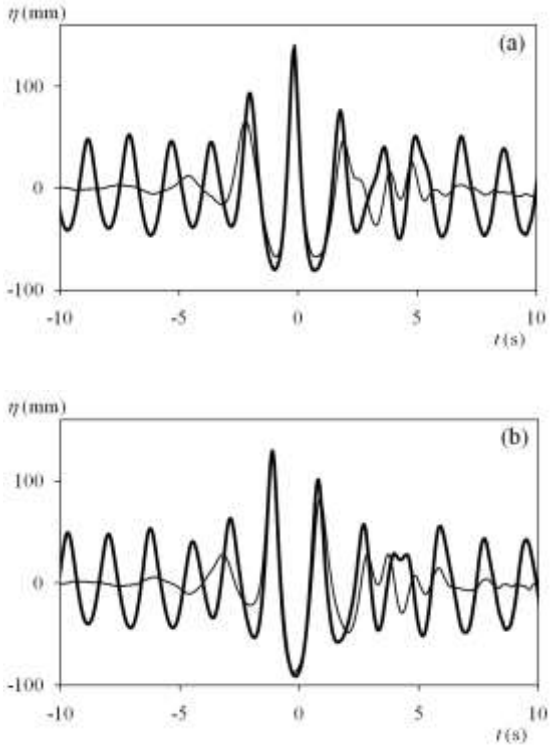


Figure 4 Superimposed time histories of embedded and lone wavegroup, for (a) EG1 and (b) EG4 (‒) embedded wavegroup, (–) lone wavegroup

*Solitary wave*

A solitary wave was also generated, which allows further investigation into the effect of wave shape on overtopping since the solitary wave has a particular form of an isolated crest with no trough. The wave was generated according to the procedure recommended by Hughes (1993) which gives a surface elevation at the paddle described by

$$\eta(x,t) = H\,\mathrm{sech}^2[\kappa(Ct - X_0)]$$

$$\eta(x,t) = H\,\mathrm{sech}^2[\kappa(Ct - X_0)] \tag{4}$$

in which $X_0$ is the paddle displacement. The constant $\kappa$ is given by

$$\kappa = \sqrt{\frac{3H}{4h^3}}$$

$$\kappa = \sqrt{\frac{3H}{4h^3}} \tag{5}$$

where $H$ is wave height and $h$ the still water depth; $C$ is the wave celerity given by

$$C = \sqrt{g(h+H)}$$

$$C = \sqrt{g(h+H)} \tag{6}$$

in which $g$ is the acceleration due to gravity. The necessary paddle signal is calculated by solving an implicit expression equating the depth-averaged horizontal fluid velocity within the solitary wave at the position of the paddle to the required velocity of the front face of the paddle. Unfortunately no closed form solution of this Lagrangian equation is possible, but numerical solution is straightforward (Hughes 1993). The solitary wave had nominal amplitude of 100 mm. Figure 5 shows the time history of the water free surface elevation 4.5 m offshore of the seawall. Table 1 lists salient details of the 13 wave cases considered herein.

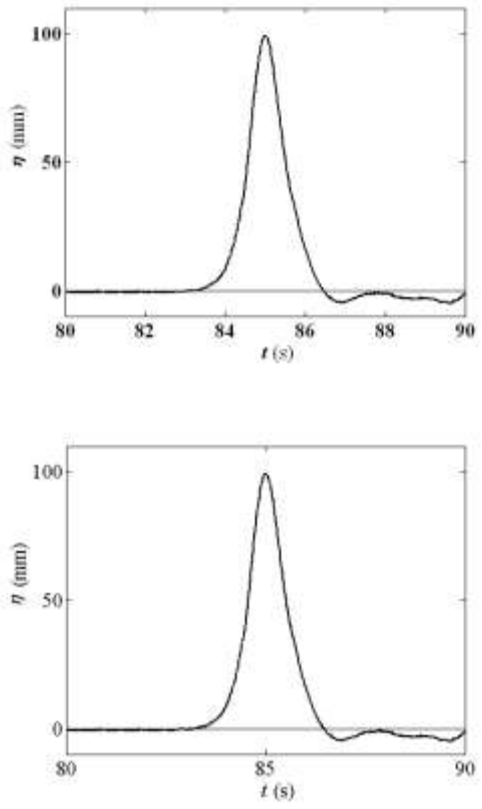


Figure 5 Surface elevation time history of solitary wave Drop all bold font from this plot, and better state 80, 85, 90 only

Table 1 Wave properties

| wave type | wave | focus location | input amplitude $A_N$ (mm) | $\phi$ (rad) | relative background wave phase (rad) |
|---|---|---|---|---|---|
| Focused wave group | WG01 | Beach toe | 114 | 0 | N/A |
| | WG02 | ¾ depth | 114 | 0 | N/A |
| | WG03 | ½ depth | 90 | 0 | N/A |
| | WG04 | Beach toe | 57 | 0 | N/A |
| | WG05 | Beach toe | 114 | π | N/A |
| | WG06 | ¾ depth | 114 | π | N/A |
| | WG07 | ½ depth | 90 | π | N/A |
| | WG08 | Beach toe | 57 | π | N/A |
| Embedded focused wave group | EG1 | Beach toe | 114 | 0 | 0 |
| | EG2 | Beach toe | 114 | π | 0 |
| | EG3 | Beach toe | 114 | 0 | π |
| | EG4 | Beach toe | 114 | π | π |
| Solitary wave | sol | N/A | 100 | N/A | N/A |

2.3 *Estimation of individual overtopping volumes*

Three methods were considered for estimation of individual overtopping volumes. The first method consisted of direct measurement of the total overtopping volume ($V_{tot\_meas}$) using a catchment area. This was constructed immediately behind a 2 m long portion of the central seawall section. A V-notch weir was cut into one side of the catchment boundary as initially it had been hoped to use the weir to determine the overtopping discharge. Tests were conducted with the V-notch open (to deduce overtopping discharge) and repeated with the notch closed (to measure total overtopping volume only). Analysis of the data suggested that the V-notch method gave inaccurate estimates of total overtopping volume, mainly due to the unsteady nature of the flow through the weir. Total overtopping volumes were therefore deduced by calibrating the catchment area using prescribed volumes of water, and measuring the distance of the wet-dry interface up the underlying 1:20 beach slope. The volume of water was measured by weight on scales accurate to ±0.05 kg, and so the water volumes used for calibration were accurate to within 0.05 l. A calibration curve was obtained that had a regression coefficient of 0.9998. This avoids errors from calculations assuming a geometrical shape which may have slight imperfections. Repeat measurements of distance up the slope, and hence the total overtopping volume, were obtained for three different wave types. Table 2 lists the results. Note that WG10 is an oblique angle wave group and WG21 a short-crested wave group, not otherwise part of the work presented here. From these results it may be inferred that the repeatability of measured volumes is to within approximately 5%.

Table 2 Repeat volume readings

| Wave Case | $V_{tot\_meas}$ (l/m) | % Error |
|---|---|---|
| WG10 | 9.42 | −1.1 |
| | 9.32 | |
| WG21 | 8.53 | +5.0 |
| | 8.96 | |
| EG1 | 36.86 | +0.6 |

| | | |
|---|---|---|
| | 37.07 | |

In the second method, overtopping volumes were estimated from water depth measurements obtained using wave gauges set into the seawall in PVC tubes (Fig. 6). Note that tubes with a closed end were embedded in the sea wall and filled with water to the level of the concrete surface before a test. This simple system enabled conventional wave probes to give time-varying water depths over the wall.

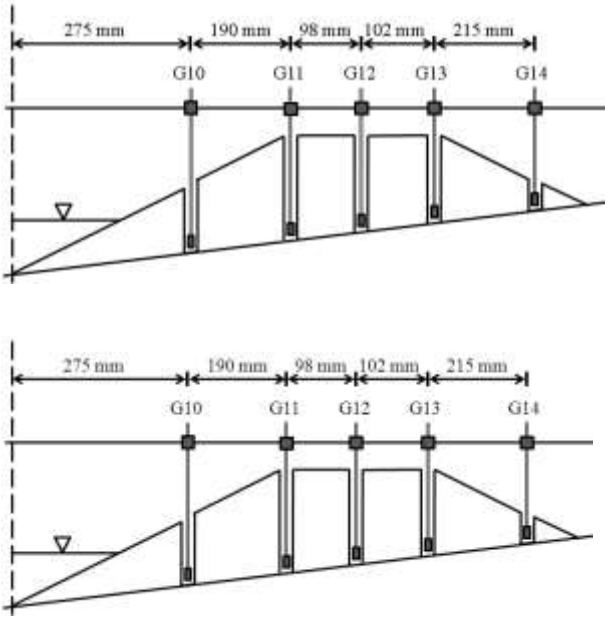


Figure 6 Placement of wave gauges in seawall, with respect to seawall toe

In practice, isolated overtopping events rarely occurred for the focused wave groups. Referring to Fig. 3, both Wave I and Wave II overtopped the structure in all test runs except for WG06 when Wave II did not overtop but additional overtopping came from two other waves in the train. To estimate the individual overtopped volumes, it was therefore necessary to interpret the wave gauge data to separate out each wave contribution. The most accurate estimates of individual overtopping volume $V_{\text{ind\_est}}$, as assessed against the total measured volumes, were obtained using the numerical time integral of the overtopping discharge $q(t)$ determined from the velocity of the overtopping wave $v(t)$ and its cross-sectional area according to

$$V_{\text{ind\_est}} = \int q(t)\,\mathrm{d}t$$

$$V_{\text{ind\_est}} = \int q(t)\,\mathrm{d}t \tag{7}$$

where

$$q(t) = v(t)\,h(t) = \sqrt{g\,h(t)}\;h(t) = g^{1/2}h^{3/2}$$

$$q(t) = v(t)\,h(t) = \sqrt{g\,h(t)}\;h(t) = g^{1/2}h^{3/2} \tag{8}$$

in which $h(t)$ is the flow depth over the seawall from wave gauges assuming unit crest length, and $g$ is the acceleration due to gravity. The maximum flow depths were 35 mm for the large amplitude crest-focused groups, of the order of 50 mm for the large trough-focused groups and 66 mm for the solitary wave. The flow velocity was predicted assuming that the flow over the top of the seawall is always at the critical condition. This assumes that the flow is quasi-steady and also that critical conditions occur at the change in slope on the top of the sea wall; both are approximations to be assessed by validation. The choice of which of the crest-mounted wave gauges to use was made by comparing preliminary predictions of total volume overtopped with experimental measurement using both seaward and landward gauges, and corresponding video footage. The landward gauge gave much smaller calculated total volumes. The video recording showed that the reason for this was that the seaward gauge interrupted the relatively shallow flow to the mid structure and landward gauges. Therefore the seaward gauge was used in all subsequent calculations. The validation of this critical flow method was undertaken for the focused wave groups and the solitary wave. Figure 7 compares the total overtopping volume estimated by summation ($V_{tot\_est}$) against the total volume measured in the catchment area, obtained for wave groups WG01 to WG08. There is satisfactory agreement between the summed and directly measured values for the smaller total overtopping volumes. However, for the larger total overtopping volumes the summed values give an underestimate of about 20%. This is believed to be due to further overtopping by reflected long waves after the surface elevation measurements had ceased. Video film of the tests confirmed that, after wave gauge data acquisition ceased, several small, reflected waves continued to overtop the seawall. In those cases, the total overtopped volume estimated by summation, based upon wave gauge data, was less than the total measured volume measured in the catchment area.

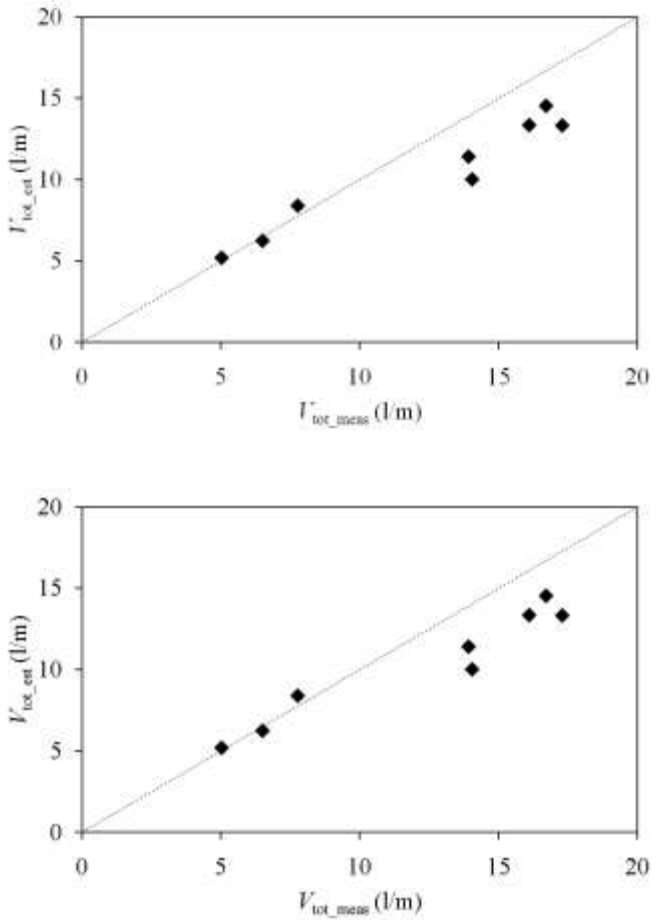


Figure 7 Comparison between total summed and directly measured wave overtopping volumes for focused wave groups

As a final check, the sum total overtopping volume was compared with the directly measured total volume for the solitary wave. Again, there was more than one overtopping contribution; a reflected wave overtopped the structure about 17 s after the main event. The wave gauge data record was sufficiently long to include this reflected wave overtopping. In this case, the total

overtopping volume estimated by summing the individual contributions was about 12% larger than the directly measured total overtopping volume.

A third, unsuccessful method, used the leading edge velocity of the overtopping wave in Eq. (8) to estimate overtopping discharge. As mentioned earlier, Schüttrumpf and Oumeraci (2005) report that the highest velocity of an overtopping wave occurs at its leading edge. This is borne out by the fact the calculated volumes based upon the leading edge velocity give considerable (up to four times) overestimates when compared with total measured overtopping volumes. In summary, the estimation method based on analysis of wave gauge data appears to give results that are sensible, and which can be used to provide insight into individual overtopping if used appropriately: i.e. where there is no effect from reflected waves.

## 3 Results

### 3.1 *Surface elevation and overtopping volume data*

Surface elevation data and individual estimated overtopping volumes are presented for the 13 normally-incident, long-crested waves in Tables 3 to 9. Results for corresponding crest- and trough-focused waves e.g. WG01 and WG05, WG02 and WG06, EG1 and EG4 etc. are listed side by side in each table. Note that Wave III is not determined for trough-focused waves as it is deemed to be insignificant in size, following two much larger waves; therefore entries for Wave III trough-focused data are denoted by (--). The locations of the surface elevation measurements in Tables 3 to 9 generally correspond to a change in geometry, though wave focal location is also included except for the case of the solitary wave. It should be noted there was no wave gauge exactly at the structure toe, therefore a gauge 125 mm seaward of the toe provided data for this location.

Table 3 Wave-by-wave surface elevation and overtopping data for WG01 and WG05 (crest-focused, trough-focused)

| | Wave I | | Wave II | | Wave III | |
|---|---|---|---|---|---|---|
| Location description (w.r.t. toe) | Crest elevation (mm) | Trough elevation (mm) | Crest elevation (mm) | Trough elevation (mm) | Crest elevation (mm) | Trough elevation (mm) |
| Offshore (−1.5 m) | 72, 155 | −20, −32 | 145, 74 | −72, -80 | 31, -- | −67, -- |
| Toe slope/ Focal point (0 m) | 61, 119 | −15, −21 | 136, 76 | −67, −86 | 42, -- | −67, -- |
| Toe structure (8 m) | 81, 107 | −9, 8 | 39, 3 | −12, −44 | −24, -- | −57, -- |
| Top structure seaward end (8.59 m) | 30, 44 | | 34, 0 | | 0, -- | |
| Top structure landward end (8.79 m) | 14, 27 | | 15, 0 | | 0, -- | |
| Overtopped volume/m (l/m) | 5.10, 11.52 | | 7.09, 0 | | 0, -- | |

Table 4 Wave-by-wave surface elevation and overtopping data for WG02 and WG06 (crest-focused, trough-focused)

| | Wave I | | Wave II | | Wave III | |
|---|---|---|---|---|---|---|
| Location description (w.r.t. toe) | Crest elevation (mm) | Trough elevation (mm) | Crest elevation (mm) | Trough elevation (mm) | Crest elevation (mm) | Trough elevation (mm) |
| Offshore (−1.5 m) | 96, 161 | 16, −50 | 124, 66 | −76, −74 | 27, -- | −65, -- |
| Toe slope (0 m) | 67, 137 | 16, −33 | 122, 70 | −77, −81 | 40, -- | −62, -- |

| | | | | | | |
|---|---|---|---|---|---|---|
| Focal point (2.5 m) | 69, 116 | 12, −22 | 147, 105 | −67, −87 | 58, -- | −64, -- |
| Toe structure (8 m) | 87, 93 | −7, 3 | 30, −15 | −17, −54 | −25, -- | −61, -- |
| Top structure seaward end (8.59 m) | 34, 43 | | 23, 0 | | 0, -- | |
| Top structure landward end (8.79 m) | 17, 28 | | 9, 0 | | 0, -- | |
| Overtopped volume (l/m) | 6.06, 11.17 | | 3.65, 0 | | 0, -- | |

Table 5 Wave-by-wave surface elevation and overtopping data for WG03 and WG07 (crest-focused, trough-focused)

| | Wave I | | Wave II | | Wave III | |
|---|---|---|---|---|---|---|
| Location description (w.r.t. toe) | Crest elevation (mm) | Trough elevation (mm) | Crest elevation (mm) | Trough elevation (mm) | Crest elevation (mm) | Trough elevation (mm) |
| Offshore (−1.5 m) | 92, 116 | −13, −53 | 85, 48 | −65, −59 | 18, -- | −50, -- |
| Toe slope (0 m) | 67, 104 | −11, −44 | 81, 51 | −68, −63 | 26, -- | −47, -- |
| Focal point (5 m) | 56, 104 | −9, −21 | 133, 116 | −53, −66 | 67, -- | −51, -- |
| Toe structure (8 m) | 73, 85 | −7, −13 | 38, −11 | −23, −54 | −17, -- | −64, -- |
| Top structure seaward end (8.59 m) | 29, 34 | | 23, 0 | | 6, -- | |
| Top structure landward end (8.79 m) | 16, 20 | | 9, 0 | | 4, -- | |
| Overtopped volume (l/m) | 4.43, 6.61 | | 3.11, 0 | | 0.35, -- | |

Table 6 Wave-by-wave surface elevation and overtopping data for WG04 and WG08 (crest-focused, trough-focused)

| | Wave I | | Wave II | | Wave III | |
|---|---|---|---|---|---|---|
| Location description (w.r.t. toe) | Crest elevation (mm) | Trough elevation (mm) | Crest elevation (mm) | Trough elevation (mm) | Crest elevation (mm) | Trough elevation (mm) |
| Offshore (−1.5 m) | 29, 63 | −11, −18 | 66, 38 | −44, −50 | 18, -- | −36, -- |
| Toe slope/ Focal point (0 m) | 25, 49 | −8, −14 | 61, 40 | −38, −51 | 19, -- | −39, -- |
| Toe structure (8 m) | 28, 64 | −12, −16 | 77, 21 | −28, −35 | 21, -- | −53, -- |
| Top structure seaward end (8.59 m) | 7, 20 | | 28, 16 | | 14, -- | |
| Top structure landward end (8.79 m) | 0, 10 | | 12, 6 | | 8, -- | |

| | | | |
|---|---|---|---|
| Overtopped volume (l/m) | 0.33, 2.52 | 3.90, 1.61 | 1.62, -- |

Table 7 Wave-by-wave surface elevation and overtopping data for EG01 and EG04 (crest-focused, trough-focused)

| | Wave I | | Wave II | | Wave III | |
|---|---|---|---|---|---|---|
| Location description (w.r.t. toe) | Crest elevation (mm) | Trough elevation (mm) | Crest elevation (mm) | Trough elevation (mm) | Crest elevation (mm) | Trough elevation (mm) |
| Offshore (−1.5 m) | 105, 145 | −37, −51 | 137, 103 | −68, −69 | 78, -- | −68, -- |
| Toe slope/ Focal point (0 m) | 77, 104 | −25, −38 | 104, 77 | −61, −71 | 55, -- | −61, -- |
| Toe structure (8 m) | 167, 119 | −18, −4 | 53, 26 | −23, −44 | −13, -- | −61, -- |
| Top structure seaward end (8.59 m) | 34, 46 | | 35, 15 | | 4, -- | |
| Top structure landward end (8.79 m) | 23, 26 | | 16, 5 | | 0, -- | |
| Overtopped volume (l/m) | 6.2, 11.2 | | 6.3, 1.1 | | 0.1, -- | |

Table 8 Wave-by-wave surface elevation and overtopping data for EG03 and EG02 (crest-focused, trough-focused)

| | Wave I | | Wave II | | Wave III | |
|---|---|---|---|---|---|---|
| Location description (w.r.t. toe) | Crest elevation (mm) | Trough elevation (mm) | Crest elevation (mm) | Trough elevation (mm) | Crest elevation (mm) | Trough elevation (mm) |
| Offshore (−1.5 m) | 93, 188 | −55, −36 | 169, 89 | −66, −81 | 103, -- | −74, -- |
| Toe slope/ Focal point (0 m) | 97, 139 | −54, −40 | 156, 84 | −76, −98 | 38, -- | −83, -- |
| Toe structure (8 m) | 33, 27 | −11, −34 | 60, 13 | −37, −41 | 3, -- | −45, -- |
| Top structure seaward end (8.59 m) | 32, 52 | | 38, 0 | | 17, -- | |
| Top structure landward end (8.79 m) | 12, 24 | | 19, 0 | | 5, -- | |
| Overtopped volume (l/m) | 6.6, 12.9 | | 9.0, 0 | | 1.5, -- | |

Table 9 Surface elevation and overtopping data for solitary wave

| Location description (w.r.t. toe) | Crest elevation (mm) |
|---|---|
| Offshore (−1.5 m) | 101 |
| Toe slope (0 m) | 88 |
| Toe structure (8 m) | 123 |
| Top structure seaward end (8.59 m) | 66 |
| Top structure landward end (8.79 m) | 31 |
| Overtopped volume/m (l/m) | 31.8 |

Overtopping severity is clearly related to the incoming wave amplitude of a sea-state and the height of individual waves. However, it also depends upon the influence of preceding waves and the intrinsic wave shape. Incoming wave amplitude and wave height are described as global influences, broadly invariant within a particular sea-state. The preceding waves and wave shape are described as being local influences on overtopping severity. Here, the local influences were investigated by varying the wave group shape (i.e. crest-focused wave group, trough-focused wave group, and solitary wave) and examining the effect of preceding waves within an embedded sequence of waves.

### 3.2 *NewWave amplitude and measured wave height*

The linear amplitude of the NewWave group indicates the size of the waves within the packet. For focused wave groups, the amplitude is defined by $A=A_N$, given in Eq. (2). Four focused wave groups (WG01, WG02, WG05 and WG06) have identical values of $A$ but different focus locations and phases. Clearly the position relative to the sea-wall and phase of the compact group will affect the subsequent wave run-up and overtopping volume. However, before examining the influence of local group structure in detail, the gross effect of incoming wave amplitude is considered. Figure 8 shows how the total overtopping volume varies as a function of the linear amplitude of the incoming wave group for all the isolated wave groups in our tests. The wave amplitude is non-dimensionalised as $A/A_{max}$, where $A_{max}$ is the size of the most energetic wave groups (WG01, 02, 05 and 06).

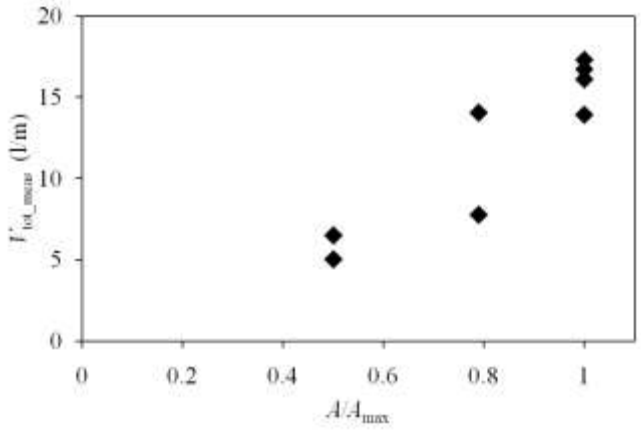

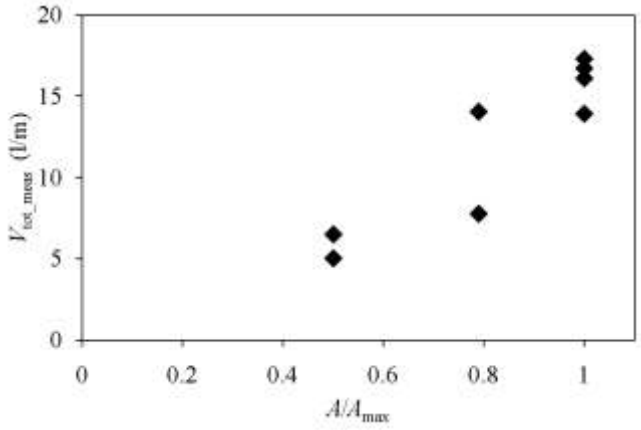


Figure 8 Measured total overtopping volume versus dimensionless NewWave amplitude

As would be expected, there is a positive correlation between total overtopping volume and non-dimensional wave amplitude $A/A_{max}$. The largest difference in total overtopping volume occurs for WG03 and WG07 where $A/A_{max} = 0.8$, with the value for WG07 (the trough-focused version of WG03) being the larger. This difference was examined using the estimated individual volumes and surface elevation time histories from the array of wave gauges. The data indicate that the crest-focused wave group, WG03, caused two significant overtopping events of 4.43 l/m and 3.11 l/m (corresponding to intra-group Waves I and II) followed by very small overtopping events. The trough-focused wave group, WG07, generated a single very large overtopping volume of 6.61 l/m corresponding to intra-group Wave I followed by further significant overtopping events.

*Measured wave height*

The relationship is now considered between the maximum height of particular waves in the group at the toe of the seawall and the individual overtopping volume due to these waves. Figure 9 shows results from Waves I and II (as defined in Fig. 3). There appears to be a cubic relationship between the individual overtopping volumes and maximum wave height measured at the toe of the structure (Fig. 9a) to be interpreted below. In absolute terms the individual overtopping volume from Wave I is usually larger than that of Wave II. However, when the overtopping volume relative to the wave height is considered Fig. 9(b) indicates that, with the exception of a single data point ($H_{toe} = 105$ mm, volume = 3.9 l/m an atypical non-breaking wave from the smallest wave group WG04), the individual overtopping volume due to Wave II is usually larger than that from Wave I, relative to its smaller wave height. It is also relevant that Wave II encounters the reflected component of Wave I as it approaches the sea wall but the effect of this interaction needs careful interpretation as the preceding wave will potentially affect both its wave height and overtopping volume.

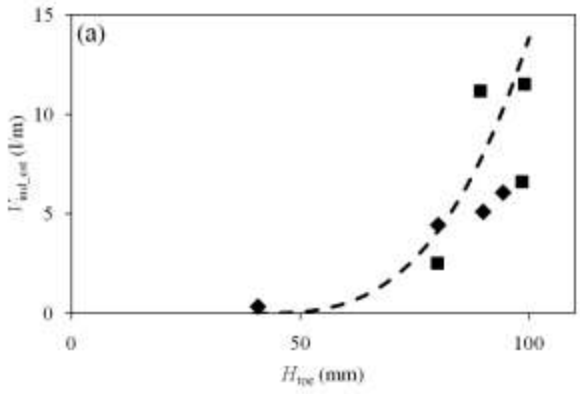

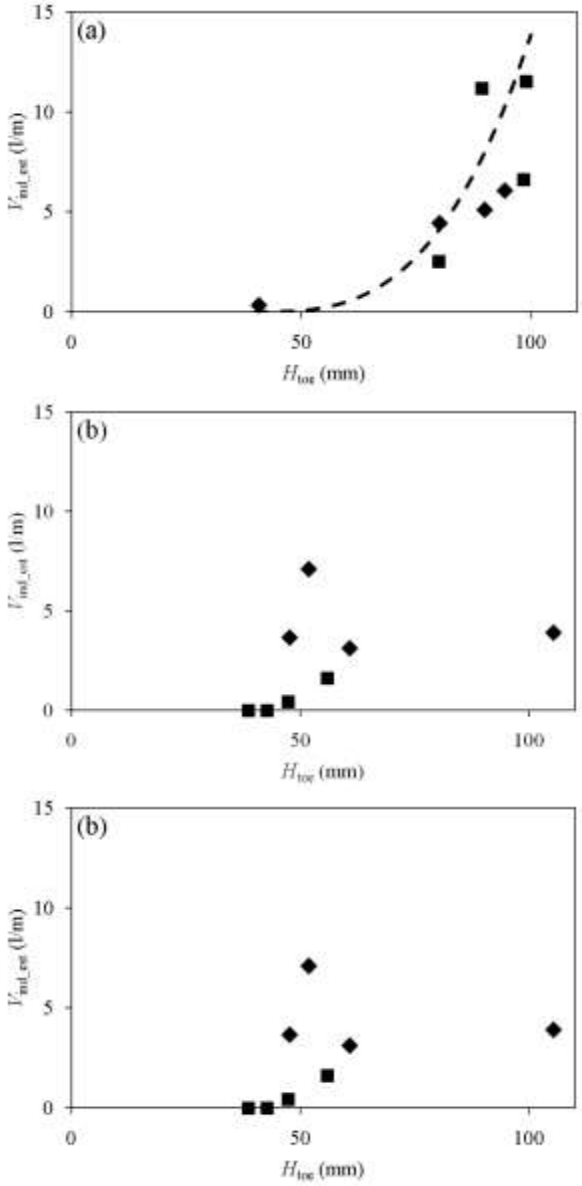


Figure 9 Individual overtopping volume versus maximum wave height at toe of sea wall for WG01 to WG08 (a) Wave I, (b) Wave II; (♦) crest-focused, (■) trough-focused, (- -) cubic fit

3.3 *Local indicators of overtopping severity – preceding waves and wave shape*

*Preceding waves*

The preceding flow field influences the interaction between an incoming wave and a coastal structure, and so overtopping due to embedded wave groups was considered. Figures 10 and 11 show free surface time histories at six locations along the centreline of the basin for a lone focused group and an embedded group, respectively. Figures 10(a) and 11(a) illustrate the near-focus situation close to the beach toe, whereas Figs. 10(f) and 11(f) relate to the top of the seawall. By this data presentation, it is confirmed that appropriate overtopping waves are being compared.

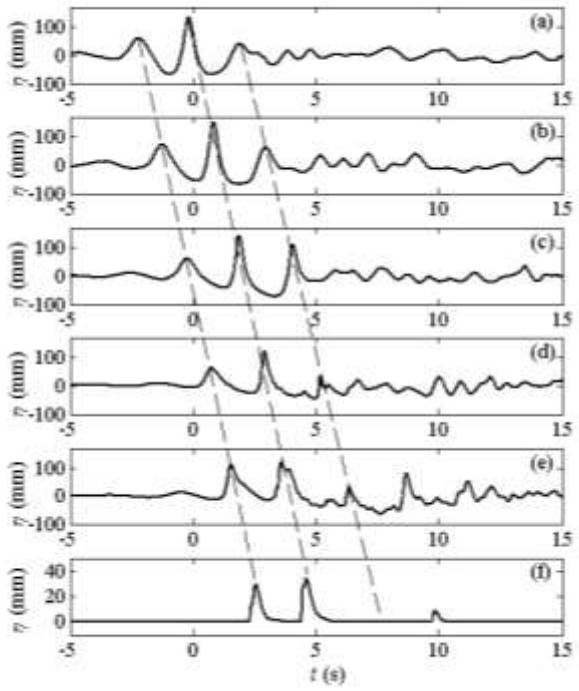


Figure 10 Surface elevation time histories of focused wave group WG01 at six locations along basin centre-line, onshore from beach toe (a) 0, (b) +2 m, (c) +4 m, (d) +5.885 m, (e) +7.25 m, (f) +8.59 m

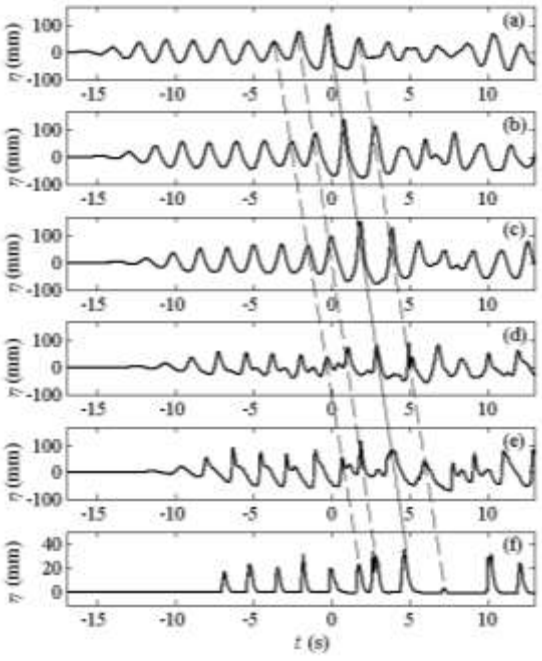

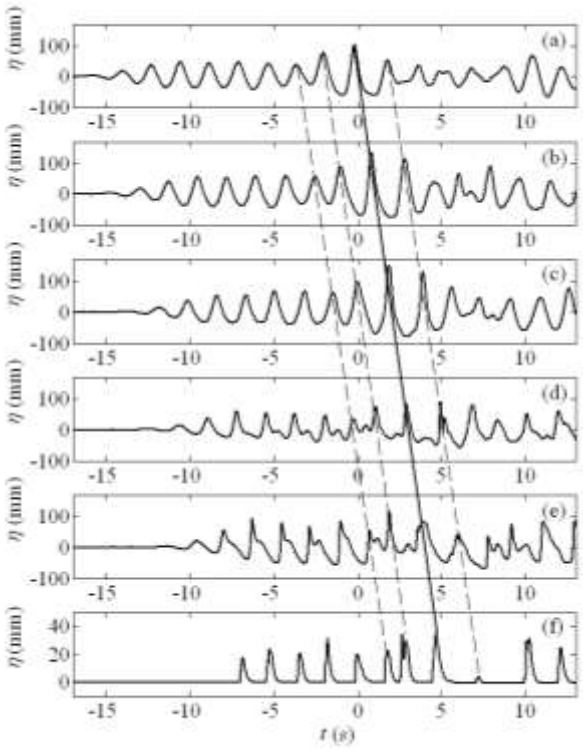


Figure 11 Surface elevation time histories of embedded wave EG1 at six locations along basin centre-line, onshore from beach toe (a) 0, (b) +2 m, (c) +4 m, (d) +5.885 m, (e) +7.25 m, (f) +8.59 m

Figure 12 shows the free surface elevation time histories of embedded and lone wave groups, measured using a wave gauge located on the seawall. For the crest-focused wave groups in Fig. 12(a), there is no significant difference between the free surface motions of lone and embedded overtopping waves. Choice of embedment of the wave group onto either the crest or a trough of a regular wave train has hardly any effect, except for a time difference of the order of a few tenths of a second for the overtopping of Wave II. An additional overtopping event occurs at about 7 s for the crest-focused wave embedded onto the trough of a regular wave, due to the succeeding regular wave crest. Figure 12(b) shows the corresponding free surface time histories obtained for the trough-focused wave groups. As for the crest-focused wave groups, there is no significant difference in the various trough-focused time histories, with and without embedment. Subsequent overtopping events from the embedded groups are again evident due to succeeding regular wave crests.

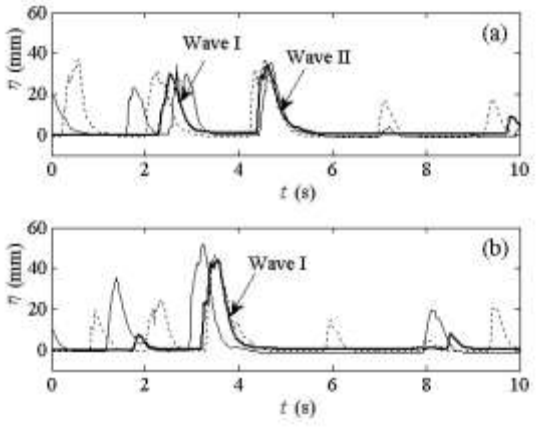

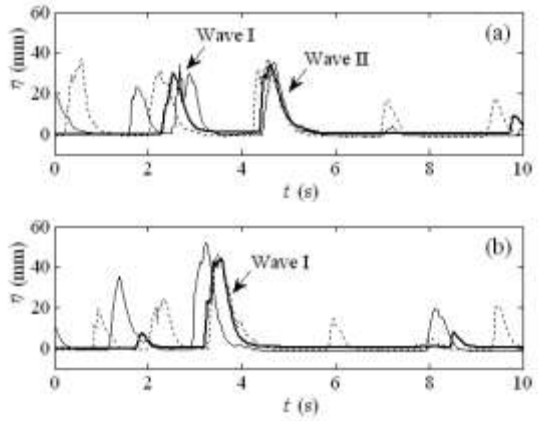


Figure 12 Surface elevation time histories at sea wall for (a) crest-focused and (b) trough-focused wave groups (▬▬) lone, (—) embedded on regular crest, (- -) embedded on regular trough

*Wave shape*

Two different types of comparisons were undertaken to explore the effect of wave shape on the overtopping volume: one using overtopping results from wave groups of opposite phase (i.e. crest-focused or trough-focused), the other comparing overtopping from focused wave groups with a solitary wave. Table 10 shows that for wave groups of the same input amplitude but opposite phase (e.g. WG01 versus WG05), the *total* measured overtopping volumes are larger for the trough-focused wave groups, except for the least amplitude groups, WG04 and WG08. Figure 13 presents *individual* overtopping volumes.

Table 10 Comparison of total measured overtopping volumes for crest- and trough-focused wave groups

| Wave pairs | $V_{tot\_meas}$ (l/m) (crest-, trough-focused wave) |
|---|---|
| WG01, WG05 | 32.2, 33.4 |
| WG02, WG06 | 27.8, 34.6 |
| WG03, WG07 | 15.6, 28.1 |
| WG04, WG08 | 13.0, 10.1 |

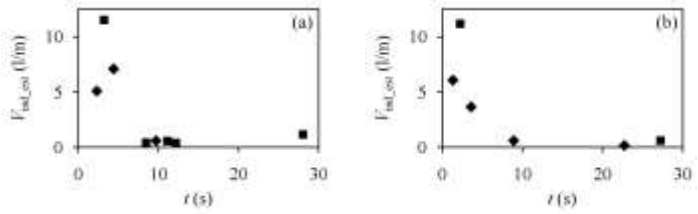

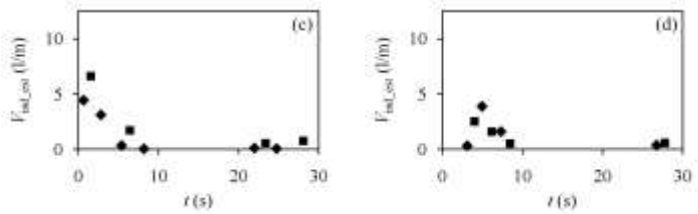


Figure 13 Overtopping volumes from individual events as function of time for (a) WG01 and WG05, (b) WG02 and WG06, (c) WG03 and WG07, (d) WG04 and WG08 with (♦) crest-focused, (■) trough-focused

The overtopping events were synchronised in such a way that Wave I overtopped at time zero for both the crest- and trough-focused groups for which the larger individual overtopping volume events tend to be due to trough-focused groups. Exceptions are WG4 and WG8, which may not be representative because of their small amplitude.

To investigate the potential effect of wave shape on overtopping, it would be desirable to compare the overtopped volume due to a solitary wave with the corresponding volume due to a focused wave. Unfortunately, no focused wave groups were produced in the UKCRF of comparable height to the solitary wave as, due to their steepness, the largest waves within the packets would break at focus. The solitary wave remained unbroken with a larger wave height due to its different structure. The overtopping volume arising due to the solitary wave is plotted in Fig. 14, an amended version of Fig. 9(a), presenting the overtopping volume from Wave I as a function of wave height at the toe of the beach, on extended axes. It appears to show that the overtopping volume of the solitary wave is comparable with the first wave in the wave group which generally caused the largest absolute overtopping volumes. Note that this finding is for one solitary wave only; it would be interesting to conduct tests to investigate this further.

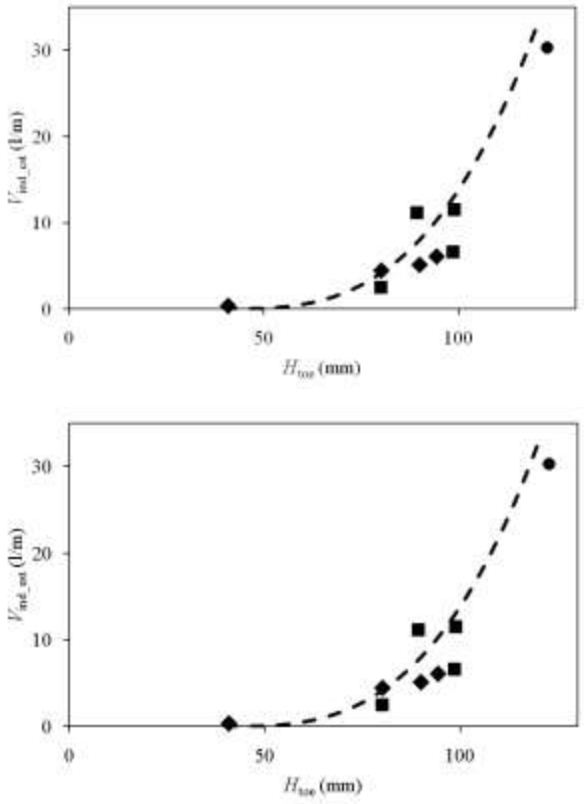

Figure 14 Individual overtopping volumes of Wave I and solitary wave versus maximum wave height at seawall toe for WG01 to WG08 with (♦) crest-focused, (■) trough-focused, (- -) cubic fit, (●) solitary wave

## 4 Discussion

### 4.1 *Estimation method*

In Section 2 a method for calculating individual overtopping volumes from wave free surface elevation time histories was described. The resulting estimates of total overtopping volumes by summation were accurate for smaller wave heights (Fig. 7). For larger wave heights, the method gave underestimates of up to 20% due in part to termination of the wave data acquisition process before the reflected, low amplitude long waves had completed reverberating and overtopping. For the solitary wave, a comparison between the total overtopping volumes obtained by summing individual wave overtopping estimates and by directly measuring the total volume gave agreement to within 12%.

### 4.2 *Overtopping data*

Surface elevation and wave overtopping volume data for eight lone focused groups, four embedded focused groups and a solitary wave are provided in Tables 3 to 9. These solitary wave data were previously used for numerical model validation by Stansby *et al.* (2008) who present overtopping volume predictions from tsunami waves using a Boussinesq model (Stansby 2003), a Volume of Fluid (VOF) model and a Smoothed Particle Hydrodynamics (SPH) model (e.g. Rogers *et al.* 2009).

### 4.3 *Effect of focused wave group height on overtopping volume*

Certain of the findings of Section 3 are intuitive: Figure 8 indicates that waves generated with larger incoming wave amplitude produce more overtopping. Figure 9 shows that there is a positive correlation between wave height measured at the toe of the structure and individual overtopping volume. The best-fit line through the overtopping volume versus $H_{toe}$ curve on Fig. 9(a) is interesting for a couple of reasons: there is an obvious intersection of the horizontal axis that implies a threshold wave height at the toe of the model seawall of around 40 mm is necessary for overtopping to occur. Also, the best-fit line follows a cubic relationship. In the literature there are no equations relating the individual overtopping volume to individual wave height; relationships are limited to overtopping *rates* described by an equation of the form (Pullen *et al.* 2007)

$$\frac{q}{\sqrt{gH_{\mathrm{m0}}^3}} = a\exp\left[-\frac{bR_{\mathrm{c}}}{H_{\mathrm{m0}}}\right]$$

$$\frac{q}{\sqrt{gH_{\mathrm{m0}}^3}} = a\exp\left[-\frac{bR_{\mathrm{c}}}{H_{\mathrm{m0}}}\right] \tag{9}$$

where $q$ is the mean overtopping discharge per meter, $H_{\mathrm{m0}}$ the spectral wave height, $R_{\mathrm{c}}$ the structure crest freeboard and $a$ and $b$ are coefficients, or maximum individual overtopping *volumes,* given by (Van der Meer and Janssen 1995)

$$V_{\max} = B\left[\ln(N_{\mathrm{ow}})\right]^{4/3}$$

$$V_{\max} = B\left[\ln(N_{\mathrm{ow}})\right]^{4/3} \tag{10}$$

where $N_{\mathrm{ow}}$ is number of overtopping waves and It also appears here that you used bold in some equations

$$B = 0.84T_{\mathrm{m}}\frac{q}{P_{\mathrm{ow}}}$$

$$B = 0.84 T_{\mathrm{m}} \frac{q}{P_{\mathrm{ow}}} \tag{11}$$

with $T_{\mathrm{m}}$ as the mean wave period and the probability of overtopping

$$P_{\mathrm{ow}} = \exp\left[ -\left( \frac{R_{\mathrm{c}}}{c H_{\mathrm{s}}} \right)^2 \right]$$

$$P_{\mathrm{ow}} = \exp\left[ -\left( \frac{R_{\mathrm{c}}}{c H_{\mathrm{s}}} \right)^2 \right] \tag{12}$$

where $c = 0.81(\gamma_{\mathrm{h}}\gamma_{\mathrm{f}}\gamma_{\beta})\xi_{\mathrm{eq}}$ in which $\gamma_{\mathrm{h}}$, $\gamma_{\mathrm{f}}$ and $\gamma_{\beta}$ are reduction factors due to a shallow foreshore, roughness and angle of wave attack, respectively, $\xi_{\mathrm{eq}}$ is the breaker parameter under the influence of a berm, and $H_{\mathrm{s}}$ the significant wave height. For these individual overtopping tests, if dimensional analysis is undertaken to identify dimensionless groups (according to the Buckingham Pi theorem) one can obtain a grouping $\Pi = VT^2g/(H^3h)$ where $V$ is individual overtopping volume, $H$ is wave height, $T$ wave period, and $h$ the crest height of the seawall with respect to the structure toe. For the present study, a cubic best-fit line is reasonable since $T$ (and $g$ and $h$) were all constant for the test cases in Fig. 9(a).

It is evident from a comparison of Fig. 9(a) with (b) that Wave I produced larger individual overtopping volumes than Wave II; however this does not give the full picture. If the smaller wave heights of Wave II are taken into consideration, it is actually Wave II that exhibits the larger overtopping volume relative to wave height at the toe of the structure. It is interesting to compare this finding with wave runup (also measured but not reported herein). Wave I generally produced the largest runup in accordance with the overtopping findings. However, Wave I also produced the largest relative runup, in contrast to the overtopping results. Looking at video recordings of the wave interacting with the beach, Wave I reduced the runup from Wave II due to downwash. Evidently Wave I does not reduce the overtopping from Wave II as there is less downwash when the water goes right over the top rather than falling back down the front of the sea wall.

To assess the earlier mentioned excessive overtopping predictions of Gunbak and Bruun (1979), it is necessary to identify successive waves in which a large wave with relatively shorter period follows a smaller wave with longer period. Referring to Fig. 3 which illustrates the intra-group waves of a focused wave group it would seem that wave pairs I and II fulfil the Gunbak and Bruun (1979) criteria for both crest and trough-focused wave groups. However, focused wave groups have this form only at the focus location; Figure 10 demonstrates the evolution of the wave group and how the size and phase of the waves are modified as the waves are influenced by the beach. Therefore it is necessary to consult the time series much closer to the sea wall structure. Figure 15 shows surface elevation time histories of wave groups WG01 to WG08; the crest-focused groups are presented at 7.25 m onshore of the beach toe, and the trough-focused group are at 5.5 m onshore of the beach toe. These locations are chosen as they correspond to the closest locations before the majority of Waves I and II break. For the crest-focused waves of Fig. 15 (a)-(d) the successive Waves I and II all have comparable periods. This is notably different from the situation at the focus location where Wave II had a shorter period. Therefore they do not satisfy the criteria for enhanced overtopping given by Gunbak and Bruun (1979). For the trough-focused waves shown in Fig. 15 (e)-(g) the periods of Waves I and II are again similar and moreover Wave II is smaller than Wave I so it would not be expected that there would be any augmentation of overtopping from the succeeding wave. The overtopping from Wave II in these focused group cases is negligible due to prior breaking. Figure 15 (h), corresponding to WG08, has a slightly shorter period Wave II compared with Wave I, and its amplitude is larger. Of the trough-focused waves, WG08 has the largest overtopping volume from Wave II even though its amplitude at focus is up to half that of the other wave groups. This appears to confirm the suggestions of Gunbak and Bruun (1979) though more detailed studies would be required to give definitive confirmation.

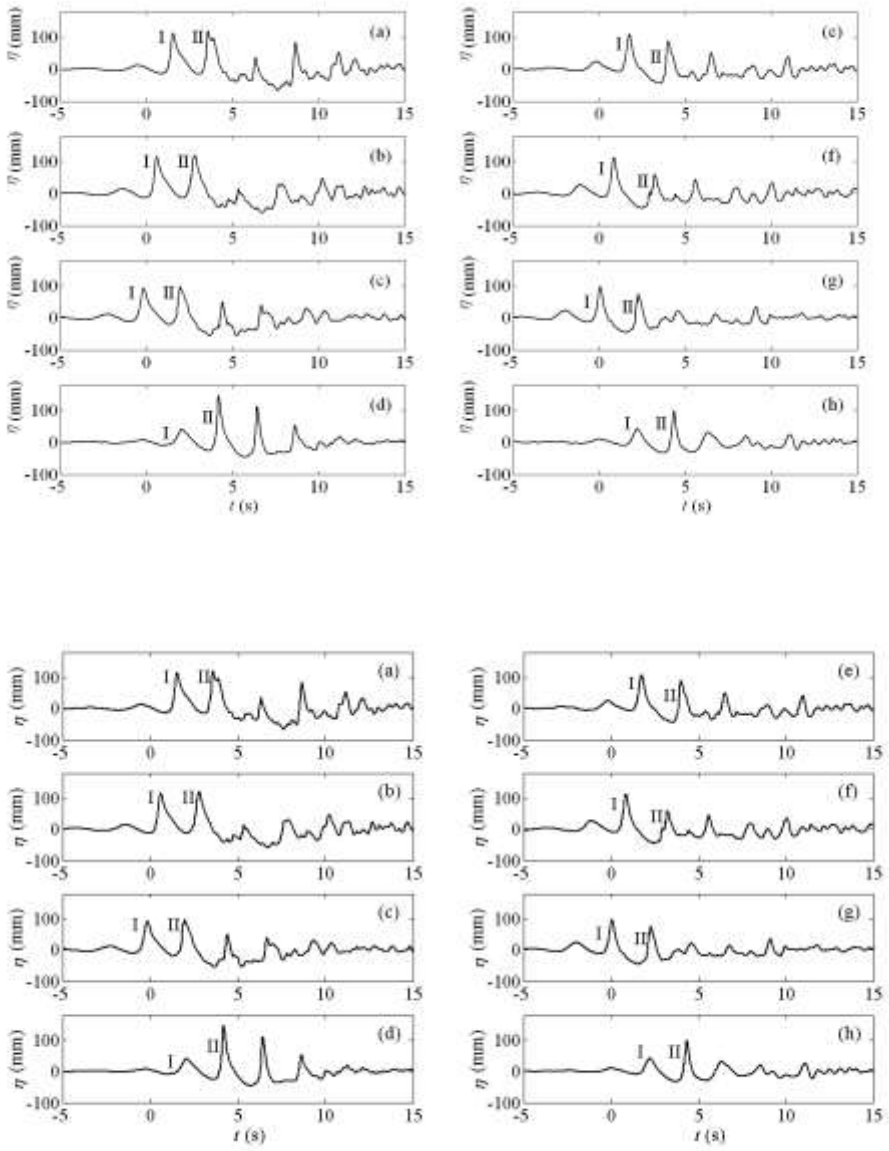


Figure 15 Surface elevation time histories of focused wave groups (a)-(d) at 7.25 m onshore of beach toe, (e)-(h) 5.5 m onshore of beach toe: (a) WG01, (b) WG02, (c) WG03, (d) WG04, (e) WG05, (f) WG06, (g) WG07, and (h) WG08

4.4 *Effect of preceding waves on overtopping volumes using embedded groups*

Use of embedded wave groups gives an opportunity to determine how carefully controlled laboratory-scale results may transfer to full-scale scenarios. Referring to Fig. 12, which shows the surface elevation time histories of the overtopping waves, there is little difference except a small phase lag. The differences are certainly less than the scatter of data presented by Tsurata and Goda (1968) which were partially due to acknowledged measurement difficulties. The findings suggest that the maximum overtopping event is hardly affected by previous waves, in keeping with the above observation that Wave II overtopping may be no smaller than Wave I overtopping (for the same wave height). This potentially makes the focused group results more transferable to practice, where wave trains are continuous.

4.5 *Effect of wave shape on overtopping volumes*

Results have been presented on the effect of wave shape on overtopping. The shape of the extreme wave was modified in two different ways by: (1) changing the phases of the wave components of the groups to give either crest- or trough-focused waves, and (2) generating a solitary wave. Waves with the same incoming wave amplitude, but of trough-focused form, generated a greater amount of overtopping than those of crest-focused form. Figure 8 shows that at $A/A_{max} = 0.8$ there are two different levels of overtopping depending on whether the wave group is crest-focused or trough-focused. Further, Table 10 shows that the overall

measured volume from the wave packet is larger for the three largest wavegroups if they are trough-focused. The only crest-focused wave that generated more overtopping was the wave group with the smallest amplitude. This finding was confirmed when the individual volumes of the overtopping waves were compared (Fig. 13): those that were generated by focusing of the troughs generated more overtopping than those generated by focusing crests; the maximum individual values were as much as 40% greater for the trough-focused groups. Again the only exception was for the smallest wave group.

The above finding may be significant as phase is not explicitly identified as being a contributory factor in overtopping; it would seem that trough-focused groups may provide worst-case scenarios for overtopping of sea defence structures. Note that Gunbak and Bruun (1979) suggest that deep troughs (which correspond to the inverted groups) may also cause considerable rundown and are therefore particularly damaging to the toes of seawalls. This finding may also shed light on the mechanics of individual overtopping events: if a deep trough produces more overtopping than a high crest (but both have identical heights), it suggests that overtopping is influenced by the depth of the water under the trough.

When the effect of wave shape was investigated by comparing individual overtopping volumes from focused wave groups with those from a single solitary wave, it was found that overtopping from a solitary wave was comparable with that from a focused group. This finding from individual wave overtopping tests is consistent with conventional overtopping formulae such as proposed by Van der Meer and Janssen (1995) which indicate that, for non-breaking waves, the dimensionless discharge and dimensionless crest height (from which overtopping discharge is determined) are independent of wave steepness. However it is slightly unexpected since runup from solitary waves on a beach (with no wall in place) was found to exceed that for focused waves (Hunt 2003). More tests need to be done to verify this for solitary waves with different characteristics.

**5 Conclusions**

A method to predict individual wave overtopping volumes by means of free surface elevation measurements over a seawall was investigated and validated against direct measurements using a catchment region. To estimate the crest velocity, it was assumed that the flow is critical at the top of the seawall. This technique gives estimates that are reasonably accurate, and is applicable to individual wave overtopping over a wide range of coastal structures, provided the crest overtopping flow conditions become critical.

For focused wave groups of different amplitudes (and hence energy spectra), the total overtopping volume and individual wave-by-wave overtopping volumes increase as the amplitude of the wave group increases. The laboratory data indicated a cubic relationship between individual wave height measured at the toe of the structure and the individual wave overtopping volume, with a cut-off presumably related to the structure freeboard.

The effect of neighbouring waves on overtopping was investigated. It was found that the overtopping event was not significantly different between lone focused and embedded focused wave groups. Moreover, the presence of a preceding primary wave did not reduce the overtopping volume contributed by the second primary wave in a focused group. The reflected first wave bulked up the second wave, augmenting the subsequent overtopping volume. This is in contrast to the attenuating effect of preceding waves on subsequent runup.

The shape of the extreme wave affects the overtopping volume. Waves of the same height at the beach toe but formed with deep troughs produced larger overtopping events than those formed with large crests. The present empirical formulae do not deal explicitly with crest-trough asymmetry. It is recommended that further research be undertaken to investigate the enhanced overtopping from trough-focused wave groups. However, wave overtopping from a solitary wave was found to be comparable with that of corresponding focused wave groups of the same amplitude, confirming conventional guidance that steepness does not influence overtopping for non-breaking waves.

**Acknowledgements**

The U.K. Coastal Research Facility was co-owned by HR Wallingford Ltd. and the U.K. Engineering and Physical Sciences Research Council. The laboratory tests were supported by EPSRC Grants GR/N21741, and GR/N22595.

**Notation**

$A$= NewWave amplitude (m) ADD dimensions to all abbreviations please

$a$ = wave amplitude (m)

$C$ = wave celerity (m/s)

$g$ = acceleration due to gravity (m/s$^2$)

$H$ = wave height (m)

$H_s$ = significant wave height (m)

$h$ = still water depth (m)

$k$ = wave number (m$^{-1}$)

$L_{op}$ = offshore wavelength (m)

$m_0$ = zero-th moment of spectrum (m$^2$)

$N$ = number of waves

$N_{ow}$ = number of overtopping waves

$P_{ow}$ = probability of overtopping

$q$ = overtopping discharge (m$^3$/s/m)

$R_c$ = structure crest freeboard (m)

$S$ = spectral energy (m$^2$.s)

$T_m$ = mean period of spectrum (s)

$T_p$ = peak period of spectrum (s)

$t$ = time (s)

$V_{tot\_est}$ = total estimated overtopping volume per unit crest width (l/m)

$V_{tot\_meas}$ = total measured overtopping volume per unit crest width (l/m)

$V_{ind\_est}$ = individual estimated wave overtopping volume per unit crest width (l/m)

$v$ = velocity of overtopping wave (m/s)

$X_0$ = paddle displacement (m)

$x$ = distance (m)

$\beta$ = structure slope

$\phi$ = phase angle (rad)

$\kappa$ = wave number of solitary wave (m$^{-1}$)

$\eta$ = surface elevation (m)

$\omega$ = wave frequency (rad.s$^{-1}$)

$\xi$= surf similarity parameter

**References**


Baldock, T.E., Swan, C., Taylor, P.H. (1996). A laboratory study of nonlinear surface waves on water. *Phil. Trans. R. Soc.* London A, 354, 649-676.

Besley, P. (1999). Overtopping of seawalls: design and assessment manual. R and D *Technical Report* W 178. Environment Agency, Bristol UK.

Bosman, G., Van der Meer, J.W., Hoffmanns, G., Schüttrumpf, H., Verhagen, H.J. (2008) Individual overtopping events at dikes. Proc. 31st Int. Conf. *Coastal Engineering* Hamburg, 2944-2956.

Burcharth, H.F., Hughes, S.A. (2006) Fundamentals of design. *Coastal engineering manual* 4, Chapter VI-5-2 Design of coastal project elements, S.A. Hughes, ed. Engineer Manual 1110-2-1100. U.S. Army Corps of Engineers, Washington DC.

Dean, R.G, Dalrymple, R.A. (1991). *Water wave mechanics for engineers and scientists*, 2nd ed. World Scientific, Singapore.

Gunbak, A.R., Bruun, P.M. (1979). Wave mechanics principles on the design of rubble-mound breakwaters. Proc. *Port and Ocean Engineering under Arctic Conditions* POAC '79, Trondheim, Norway, 1301-1318.

Hughes, S. (1993). *Physical models and laboratory techniques in coastal engineering*. Advanced Series in Ocean Engineering 7. World Scientific, Singapore.

Hunt, A.C. (2003). Extreme waves, overtopping and flooding at sea defences. *D.Phil. Thesis*. Oxford University, Oxford UK.

Jonathan, P., Taylor, P.H. (1997). On irregular, nonlinear waves in a spread sea. *J. Offshore Mechanics and Arctic Engineering* 119(1), 37-41.

Kortenhaus, A., Oumeraci, H., Geeraerts, J., De Rouck, J., Medina, J.R., Gonzalez-Escriva, J.A. (2004). Laboratory effects and further uncertainties associated with wave overtopping measurements. Proc. 29th Int. Conf. *Coastal Engineering* Lisbon, 4456-4468.

Lindgren, G. (1970). Some properties of a normal process near a local maximum. *Annals of Mathematical Statistics* 41(6), 1870-1883.

Pearson, J., Bruce, T., Allsop, N.W.H. (2002). Violent wave overtopping: measurements at large and small scale. Proc. 28th Int. Conf. *Coastal Engineering* Cardiff, 2227-2238. ASCE, Reston VA.F

Pullen, T., Allsop, N.W.H., Bruce, T., Kortenhaus, A., Schüttrumpf, H., Van der Meer, J.W. (2007). *EurOtop*: Wave overtopping of sea defences and related structures: Assessment manual. www.overtopping-manual.com.

Richardson S., Pullen T., Clarke S. (2002). Jet velocities of overtopping waves on sloping structures: Measurements and computation. Proc. 28th Int. Conf. *Coastal Engineering* Cardiff, 2239-2250.

Rogers, B.D., Dalrymple, R.A., Stansby, P.K. (2009). Simulation of caisson breakwater movement using SPH. *J. Hydraulic Res.* 47(Extra Issue), 135-141.

Schüttrumpf, H.F.R., Oumeraci, H., Möller, J., Kudella, M. (2001). *Loading of the inner slope of seadikes by wave overtopping*. *Report* 858 Leichtweiss Institut für Wasserbau, Technische Universität Braunschweig, Germany.

Schüttrumpf, H., Oumeraci, H. (2005) Layer thicknesses and velocities of wave overtopping flow at seadikes. *Coastal Engineering* 52(6), 473-495.

Stansby, P.K. (2003). Solitary wave runup and overtopping by a semi-implicit finite-volume shallow-water Boussinesq model. *J. Hydraulic Res.* 41(6), 639-648.

Stansby, P.K., Xu, R., Rogers, B.D., Hunt, A.C., Borthwick, A.G.L., Taylor, P.H. (2008). Modelling tsunami overtopping of a sea defence by shallow-water Boussinesq, VOF and SPH methods. *Floodrisk* 2008 Oxford UK, 255-261.

Tautenhain, E., Kohlhase, S., Partenscky, H.W. (1982). Wave run-up at sea dikes under oblique wave approach. Proc. 18th Int. Conf. *Coastal Engineering* Cape Town, 804-810.

Taylor, P.H., Jonathan, P., Harland, L.A. (1997). Time domain simulation of jack-up dynamics with the extremes of a Gaussian process. *J. Vibration and Acoustics* 119(4), 624-628.

Taylor, P.H., Williams, B.A. (2004). Wave statistics for intermediate depth water: NewWaves and Symmetry. *J. Offshore Mechanics and Arctic Engineering* ASME 126(1), 54-59.

Troch, P., Geeraerts J., Van de Walle, B., Rouck, J., Damme, L., Allsop, W., Franco, L. (2004). Full-scale wave overtopping measurements on the Zeebrugge rubble mound breakwater. *Coastal Engineering* 51(7), 609-628.

Tromans, P.S, Anaturk, A., Hagemeijer, P. (1991). A new model for the kinematics of large ocean waves: Application as a design wave. Proc. 1st Int. Conf *Offshore and Polar Engineering* Edinburgh UK 3, 64-71.

Tsuruta, S., Goda, Y. (1968). Expected discharge of irregular wave overtopping. Proc. 11th Conf. *Coastal Engineering* London, 833-852. ASCE, New York.

Van der Meer, J.W., Janssen, P.F.M. (1995). Wave run-up and wave overtopping at dikes. Wave forces on inclined and vertical wall structures, 1-26, Z. Demirbilek, ed. ASCE, New York.

Van Gent, M.R.A. (2002) *Low-exceedance wave overtopping events*. WL Delft project id DC030202/H3803. Delft Hydraulics, Delft NL.

[Stansby (2003) **and Rogers et al. (2009)** added] Yes, but this is self-citation…

[We did a thorough search back to 2005/6 and found 3 potentials: one by Pontillo et al. and Schmocker and Hager deal with dyke erosion by overtopping and a paper by Crespo et al. would have been appropriate to cite if we had been dealing with numerical modelling of wave overtopping. We therefore conclude that there is nothing of direct relevance aside from the self-cited papers now included. Are there any others in the special edition that would be relevant?] Schmocker and Hager (2009) do NOT deal with numerical methods. For other papers in the current SI, you better have a check with Prof. Memos